JOURNAL OF MATERIALS SCIENCE 24 (1989) 88–96

Grain boundary resistivity in Y-TZP materials as a function of thermal history

S. P. S. BADWAL, J. DRENNAN
Division of Materials Science and Technology, CSIRO, Normanby Road, Clayton, Victoria 3168, Australia

Grain-boundary resistivity in yttria-containing tetragonal zirconia polycrystalline (Y-TZP) materials dominates the total resistivity. Impedance measurements combined with microstructural studies suggest that post-sintering heat treatments (in particular the cooling rate) influence the location of the grain-boundary phase which, in turn, has a significant effect on the grain-boundary resistivity. Higher cooling rates from the sintering temperature lead to reduction in the grain-boundary resistivity. In both alumina-containing and relatively pure tetragonal zirconia polycrystals, post-sintering heat treatments have a less conspicuous effect. The activation energy associated with the grain-boundary resistivity was independent of the post-sintering heat treatments but was 25 to 30 kJ mol^{-1} higher than that for the oxygen-ion conduction within the grains at low temperatures.

1. Introduction

With the combination of high strength (1 GPa flexural strength) [1] and an ionic conductivity better than that of fully stabilized zirconia below 600° C [2], yttria-containing tetragonal zirconia polycrystalline (Y-TZP) materials are an increasingly attractive proposition for application as electrolyte materials in devices such as fuel cells, oxygen pumps and electrochemical reactors. However, the limiting factor in using these ceramics in oxygen-ion conducting devices is that their small grain size (0.5 to 2 μm), which is necessary for high strength, results in a material with a large total grain-boundary area. This, in conjunction with the omnipresent glassy grain-boundary phases, give rise to the materials having an unacceptably high grain-boundary component in the total resistivity of the sample.

To minimize grain-boundary resistivity without interfering with the mechanical strength of the ceramic it is necessary to modify the nature of the grain boundaries in such a way as to make the passage of oxygen ions as easy as possible. Additions of Al_2O_3 [3, 4] have been shown to be successful in this regard by effectively removing the insulating grain-boundary phase by reaction.

In this paper we investigate the effect of post-sintering thermal treatments on both the grain-boundary and volume resistivity of 3 mol % Y_2O_3 + 97 mol % ZrO_2 and 80 wt % (3 mol % Y_2O_3 + 97 mol % ZrO_2) + 20 wt % Al_2O_3. To determine the mechanism by which the thermal history affects the grain-boundary resistivity, we have combined extensive microstructural analysis with a.c. impedance spectroscopy.

2. Experimental procedures

The materials used in this study were: (1) 3 mol % Y_2O_3 + 97 mol % ZrO_2 (TZ3Y-00A) and (2) 80 wt % (3 mol % Y_2O_3 + 97 mol % ZrO_2) + 20 wt % Al_2O_3 (TZY3-20A). Prereacted powders of both compositions were obtained from Toyo Soda Ltd, Japan. These powders have been quoted by the manufacturer to contain impurities such as silica. Both powders were isostatically pressed into discs and sintered at 1500° C for 4 h in atmospheric air. For all firings except where the effect of heating rate was studied, the specimens were heated at a rate of 300° C h^{-1} to the sintering temperature. The cooling rate was varied from 50° C h^{-1} to several thousand ° C h^{-1} (air quench). Table I gives nomenclature, composition and thermal history.

In addition to those listed in Table I, some TZ3Y-00A specimens were cooled to 1300° C from the sintering temperature at the slowest cooling rate (Table I), held for 0.5 h at 1300° C and then quenched. Other post-sintering heat treatments included: taking the slowly cooled specimens to 1500° C at the heating rate of 300° C h^{-1}, holding for 10 to 30 min followed by quenching; and taking previously quenched specimens to 1500° C and cooling at the slowest rate. In addition, several previously quenched specimens were re-heated at 300° C h^{-1} and held for a period of time between 900 and 1300° C before being subjected to a further quench.

The sintered discs had a diameter of about 9.5 to 9.7 mm, thickness between 3.0 and 3.2 mm and density > 98% theoretical.

For impedance measurements, the surface of the as-fired samples was ground gently with silicon carbide powder. The discs were cleaned and coated with low-impedance electrodes consisting of a mixture of platinum and a urania–scandia fluorite solid solution [5]. The impedance data were collected over the temperature range 375 to 600° C. In addition to the previously described heat treatments, specimens which had been quenched were subjected to various

0022–2461/89 $03.00 + .12 © *1989 Chapman and Hall Ltd.*

TABLE I Specimen preparation details

Nomenclature for alumina-free specimens	Nomenclature for alumina-containing specimens	Sintering temperature, °C (time, h)	Heating rate (°C h^{-1})	Cooling rate (°C h^{-1})
TZ3Y-00A151	TZ3Y-20A151	1500(4)	300	50
TZ3Y-00A152	TZ3Y-20A152	1500(4)	300	100
TZ3Y-00A153	TZ3Y-20A153	1500(4)	300	200
TZ3Y-00A154	TZ3Y-20A154	1500(4)	300	300
TZ3Y-00A156	TZ3Y-20A156	1500(4)	300	Quenched
TZ3Y-00A155	TZ3Y-20A155	1500(4)	50	100
PTZ3Y-00A154*	–	1500(4)	300	300
PTZ3Y-00A156*	–	1500(4)	300	Quenched

*Except for these two, all other specimens were prepared from powders supplied by Toyo Soda Ltd.

heat cycles in the impedance furnace. These included slow cycling from room temperature or 350° C to a temperature in the 750 to 900° C range. The samples were held for several hours at the peak temperature and then cooled, at which stage, impedance spectra were recorded at several temperatures. The frequency range of the measurements was 1 Hz to 1 MHz. In all, more than 25 specimens were studied.

The microstructure of selected specimens was examined with both scanning and transmission electron microscopes. Transmission electron microscopy samples were prepared by ion-beam thinning 3 and 2 mm diameter discs cut from the central regions of selected specimens. For scanning electron microscopy examination, specimens were polished and thermally etched. To avoid charging problems, specimens were coated with a 20 nm layer of carbon. Microscopes used were a Hitachi S-450LB scanning electron microscope, a Philips 420 for analytical transmission electron microscopy and, for high resolution studies, a Jeol 200CX.

X-ray diffractograms were recorded both on as-fired and ground surfaces. For elemental analysis of the surfaces of quenched and slow cooled specimens, electron spectroscopy for chemical analysis (ESCA) was used.

3. Results

3.1. Impedance measurements

Fig. 1 shows impedance diagrams for specimens from both TZ3Y-00A and TZ3Y-20A compositions for three cooling cycles. Materials which were cooled at intermediate rates between those plotted had intermediate total resistivities. The materials free of alumina show a dramatic reduction in the total resistivity due to increased cooling rate. This change is almost entirely a result of the change in the grain-boundary resistivity, R_{gb} (the arc on the right-hand side in Fig. 1). The volume resistivity of the quenched specimens was slightly lower (by about 10 to 20%) compared with the slowly cooled samples. Similar behaviour for the grain-boundary resistivity has been reported by Leach *et al.* [6] for materials of the TZ3Y-00A composition.

For materials containing Al_2O_3 (Fig. 1b), the effect is far less dramatic. However, it should be noted that the addition of Al_2O_3 has already served to modify R_{gb} [3, 4], reducing the total resistivity almost two-fold from its Al_2O_3-free counterpart.

The effect of different heating rate on identical samples is shown in Fig. 2. These specimens were heated at a rate of 50 and 300° C h^{-1}, respectively, to the sintering temperature (1500° C) and then cooled at the same rate of 100° C h^{-1}. Despite a six-fold increase in the heating rate, the resistivities of both specimens are virtually identical.

In order to check if the effect of slow cooling or quenching could be reversed, the sintered specimens which were originally cooled at the rate of 100° C h^{-1} (TZ3Y-00A152) were taken back to 1500° C, held for

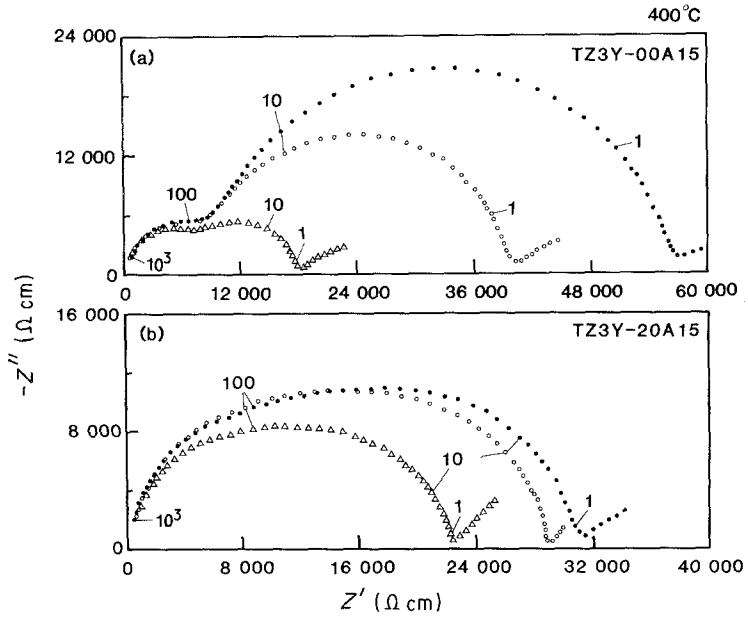

Figure 1 Impedance diagrams for (a) TZ3Y-00A15 and (b) TZ3Y-20A15 specimens at 400° C showing the grain-boundary (right) and volume (left) resistivity arcs. Heating rate: 300° C h^{-1} for all specimens. Cooling rate: (●) 50° C h^{-1}, (○) 300° C h^{-1}, (△) air quench. The numbers on the arcs in this and Figs 2 to 7 are frequencies in kHz.

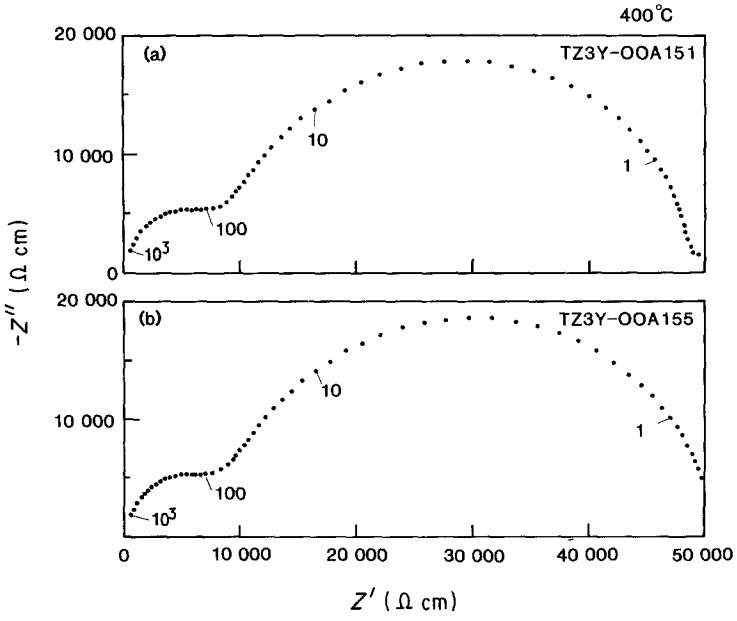

Figure 2 Impedance diagrams at 400° C showing the effect of different heating rates for TZ3Y-00A15 specimens. Cooling rate 100° C h^{-1} for both. Heating rate: (a) 300° C h^{-1} and (b) 50° C h^{-1}.

10 min and quenched (TZ3Y-00A152(6)). Conversely, the reverse treatment (a slow cool) was given to specimens which had been previously quenched (TZ3Y-00A156) from the sintering temperature. Fig. 3 summarizes these results. The TZ3Y-00A156 specimens on slow cooling from 1500° C (TZ3Y-00A156(2)) showed a considerable increase in the grain-boundary resistivity but the final value observed was lower than that of the TZ3Y-00A152 specimen. The slowly cooled specimens showed a considerable drop in the grain-boundary resistivity on quenching from 1500° C. The final value in this case was only slightly higher than that of TZ3Y-00A156.

TZ3Y-00A specimens cooled at the rate of TZ3Y-00A151 from the sintering temperature of 1500 to 1300° C, held for 0.5 h and then quenched (TZ3Y-00A15136) showed no change in R_{gb} but exhibited slightly higher volume resistivity when compared with specimens quenched directly from 1500° C (Fig. 4). Also specimens cooled rapidly from 1500 (TZ3Y-00A156) or 1300° C (TZ3Y-00A15136) when annealed at 900° C for 11 h (Fig. 5) and 1100° C for 10 h (Fig. 6), respectively, and then quenched from the annealing temperature, showed only small increase in the grain-boundary (< 20%) and volume (< 10%) resistivities. This change in the grain-boundary resistivity is insignificant compared with that observed between slowly cooled and quenched samples.

Fig. 7 compares the impedance spectrum of a Toyo Soda TZ3Y-00A154 specimen (heating and cooling rates 300° C h^{-1}, sintered at 1500° C for 4 h) with that of a high purity material of the same composition which had been given an identical heat treatment (PTZ3Y-00A154). This high purity material was obtained from an alternative source to Toyo Soda and had a measured impurity level of < 100 p.p.m. The grain-boundary resistivity of the pure material is seen to be much lower than that of the Toyo Soda specimen. In fact the grain-boundary resistivity of PTZ3Y-00A154 was comparable with that of the Toyo Soda quenched material. In addition the cooling rates were observed to have only a small effect on the grain-boundary resistivity of this pure material.

The activation energy associated with the grain-boundary resistivity was independent of the cooling rate but was 25–30 kJ mol^{-1} higher than that for

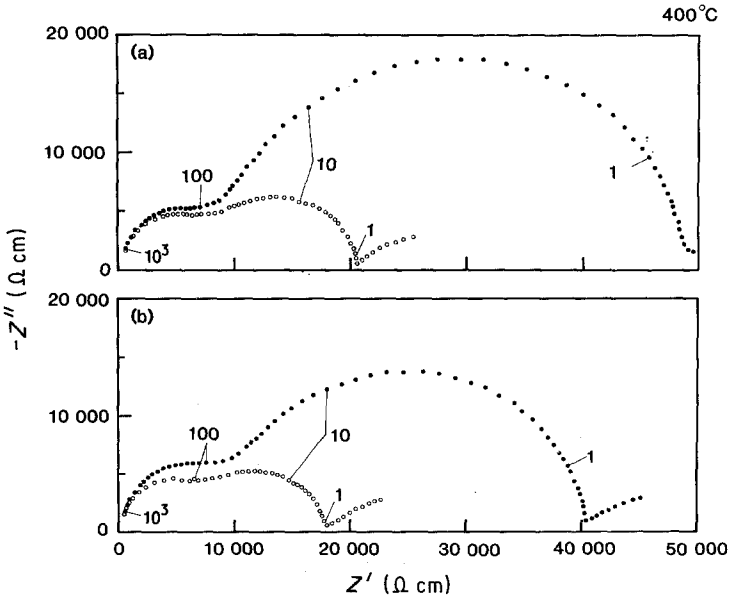

Figure 3 Impedance spectra at 400° C for TZ3Y-00A15 samples. (a) (●) TZ3Y-00A152, (○) same specimen after it had been taken to the sintering temperature and quenched. (b) (○) TZ3Y-00A156, (●) same specimen after it had been taken to the sintering temperature and cooled at the rate of 100° C h^{-1}.

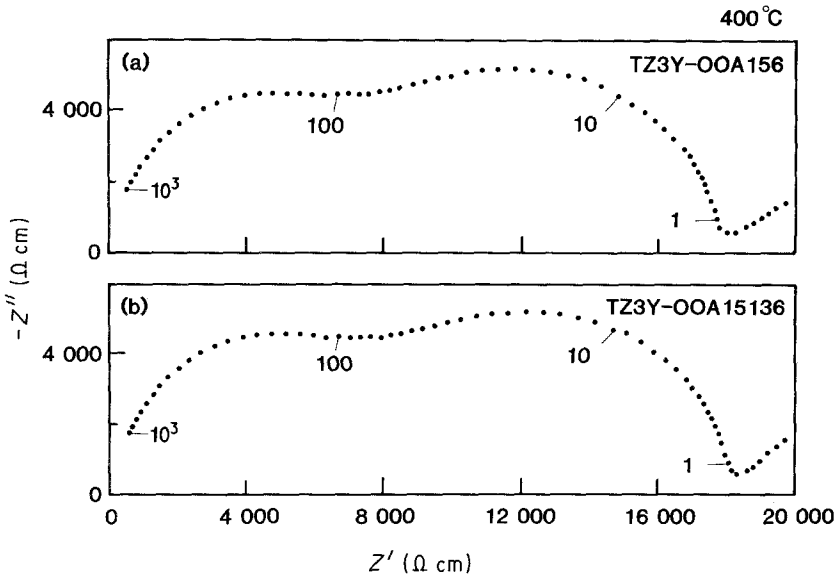

Figure 4 Impedance spectra at 400° C for (a) a specimen quenched from the sintering temperature, (b) a specimen first slowly cooled to 1300° C from the sintering temperature, held for 0.5 h and then quenched.

oxygen-ion conduction within the grains at low temperatures (375 to 450° C).

3.2. Microstructure/characterization

Microstructural examination of selected specimens was undertaken to determine if any effects of the different cooling rates could be observed. In the first instance, no change in grain size or extent of exaggerated grain growth was observed as a function of the cooling rate (Fig. 8). This was the case for both alumina-free and alumina-containing samples. In each of these sets of specimens the microstructure at this level of magnification appears to be identical. Further to this, TZ3Y–00A151 and TZ3Y–00A156 samples were examined using transmission electron microscopy.

Attention was paid to the grain-boundary phases which accumulate at triple-point junctions in both samples. Energy dispersive X-ray spectra were recorded from up to 15 different triple-grain junctions in each sample in order to determine if any chemical changes resulted from the differing cooling rates. Although minor differences in the chemical composition were detected between slowly cooled (TZ3Y–00A151) and rapidly quenched (TZ3Y–00A156) specimens, they were within the experimental limits of detection to draw any definitive conclusions. The grain-boundary phases in both samples were amorphous and consisted of predominantly silicon with an enriched yttrium content compared to the surrounding Y–TZP grains. Examples of the typical energy dispersive X-ray spectra are shown in Fig. 9.

To investigate further the nature of the grain-boundary phase, high-resolution electron microscopy was used to examine the grain boundaries of the quenched and slowly cooled samples. Although the triple-grain junctions and grain boundaries in both sets of samples appeared identical on the atomic scale, two observations of a general nature concerning these types of ceramic were made. Firstly, the grain-boundary phase did not coat all grains uniformly. Numerous examples of grain boundaries with atom to atom contact between adjoining grains were observed and examples of such boundaries are shown in Fig. 10. We believe this is a significant observation, because it has been suggested by previous workers that the grain-boundary glassy phase totally coats all grains of this type of ceramic [7, 8]. This has important

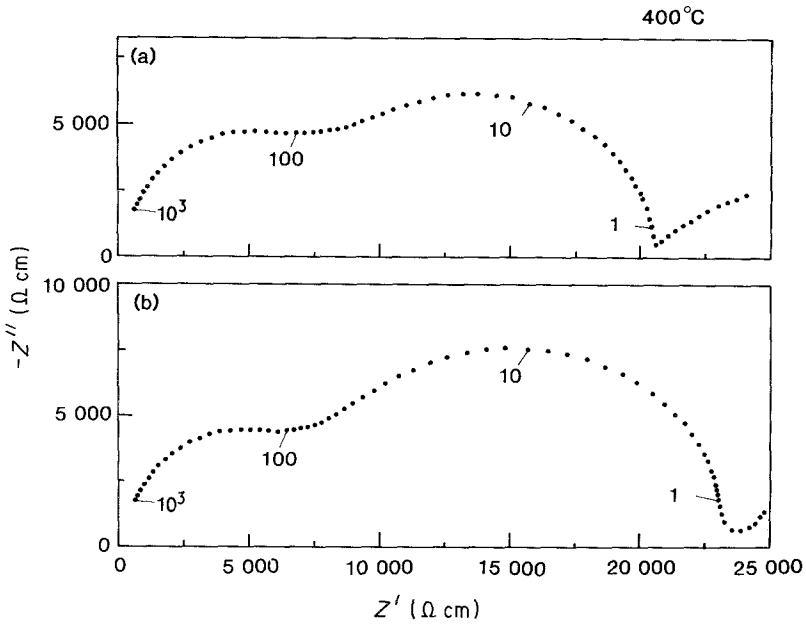

Figure 5 Impedance diagrams at 400° C for a specimen quenched from the sintering temperature of 1500° C (a) before annealing and (b) after annealing at 900° C for 11 h and quenching.

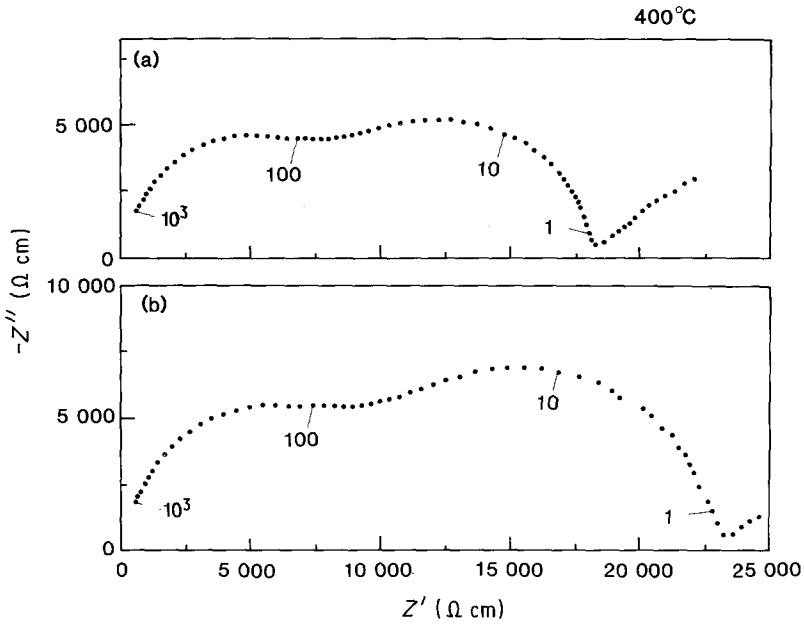

Figure 6 Impedance diagrams at 400° C for (a) a specimen as in Fig. 4b and (b) same specimen after annealing at 1100° C for 10 h and quenching.

consequences in explaining some of the effects we observe concerned with the differing heat treatment. The glass phase is insulating, hence the more it is removed or restricted to isolated pockets the less hindered are the diffusing oxygen ions. The second observation is that the interface between the accumulated glass phase of the triple-grain junction and the surrounding grain is not straight, but contain atomic steps. Clarke [9] has suggested that the observation of such steps may be a necessary criterion to account for the de-wetting processes occurring in ceramic systems.

To this stage no quantitative differences in any microstructural features were measured between the materials subjected to different cooling rates. Qualitatively, triple-grain junctions containing glassy phases were more numerous in materials which had been subjected to a rapid quench.

A difference in the composition of the as-fired surfaces between TZ3Y-00A15 materials which had been quenched and materials which had been slowly cooled was detected by electron spectroscopy (ESCA). The yttrium/zirconium ratio in slowly cooled specimens was about 1.5 times that observed in the quenched specimen. Moreover, monoclinic zirconia was detected by X-ray diffraction at the surface of materials free of alumina but which had been subjected to a slow cool. In alumina-containing specimens the amount of surface monoclinic zirconia was relatively small and the high-purity sample, designated PTZ3Y, showed no evidence of monoclinic zirconia irrespective of the cooling rate.

In summary, our observations are as follows.

1. Fast cooling rates from the sintering temperature improve the total ionic conductivity of Y-TZP materials by reducing the grain-boundary resistivity.

2. Materials containing Al_2O_3 do not show the same effect and neither does a Y-TZP material with a very low impurity content.

3. Heating rate to the sintering temperature does not affect the ionic conductivity of any of these samples.

4. Previously quenched samples, when subjected to a slow cool from the sintering temperature, show an increase in the grain-boundary resistivity. Conversely, when slowly cooled specimens were taken back to the sintering temperature and quenched they

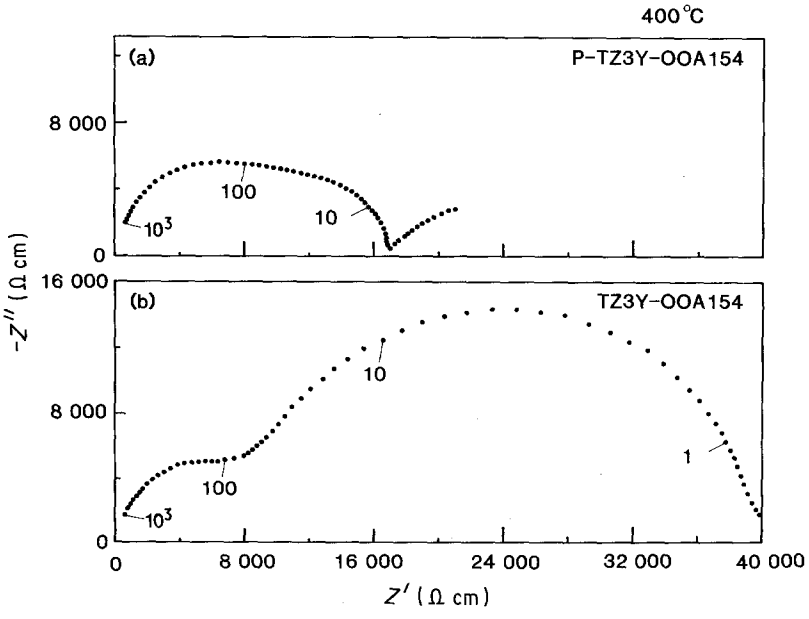

Figure 7 Impedance diagrams at 400° C for (a) pure TZ3Y and (b) Toyo Soda TZ3Y specimens. For both materials sintering temperature: 1500° C (4 h); heating and cooling rates 300° C h^{-1}.

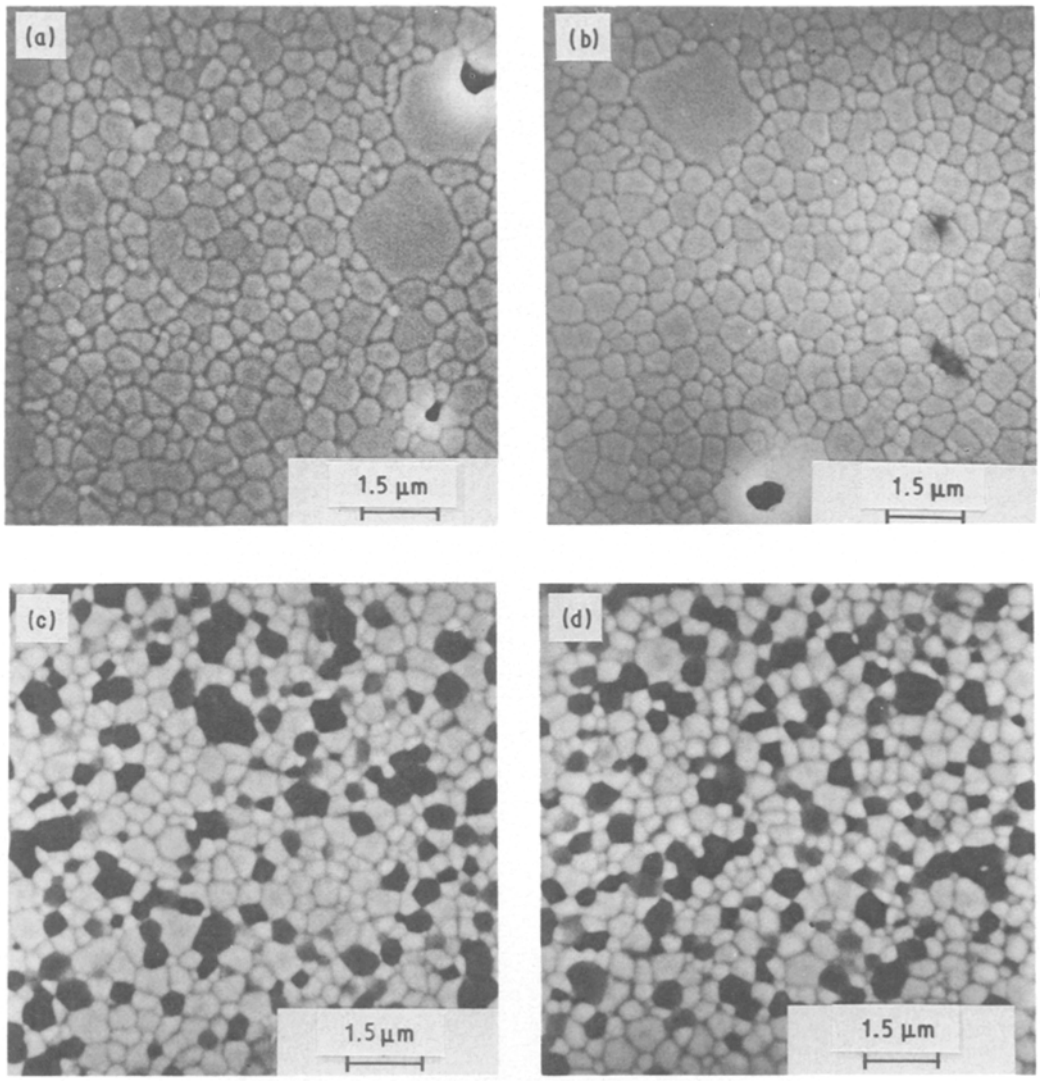

Figure 8 Scanning electron micrographs for TZ3Y specimens: (a) quenched, no Al_2O_3, (b) slowly cooled no Al_2O_3, (c) quenched, with Al_2O_3, and (b) slowly cooled, with Al_2O_3.

showed a considerable decrease in the grain-boundary resistivity.

5. Previously quenched specimens when either (1) annealed at a temperature between 900 and 1300° C and quenched, or (2) slowly cycled between room temperature or 350° C and 750 to 900° C, showed only a small increase in the grain-boundary resistivity.

6. No changes in the composition of the grain-boundary phase as a function of thermal history were detected.

7. Not all grain boundaries are coated with a secondary glassy phase and atomic steps were observed at grain boundaries.

4. Discussion

From the results presented it is clear that the differences in the total resistivity as a function of the cooling rate, which were observed for Y–TZP and Y–TZP containing 20 wt % Al_2O_3, are a result of changes occurring at or near the grain boundaries. We suggest that two possibilities exist to explain the observed differences in the grain-boundary resistivity as a result of different cooling rates.

4.1. Chemical changes at or near the grain boundaries

At this composition (3 mol % Y_2O_3) and grain size, the ceramic under investigation is in a metastable state. The system will tend to disproportionate into a high and low yttria content diphasic material with grains having cubic and tetragonal or monoclinic symmetry, respectively. In doing so it will lead to a situation where yttrium concentration gradients within the grains are likely to be present. These processes are further complicated by the presence of grain-boundary phases which have been shown to be the medium through which redistribution of yttrium occurs [10]. Previous authors [7, 11] have reported intragrain composition variation in yttria–tetragonal zirconia polycrystals; the yttrium concentration being higher near the grain-boundary region. In our work, minor differences in yttrium concentration across grains were also observed. It could be suggested that enrichment of yttrium at the grain surfaces will lead to a layer of less-conducting material surrounding each grain. However, this can be discounted, because the ionic conductivity of Y_2O_3–ZrO_2 compositions containing 2, 3, 4, 6 and 8 mol % Y_2O_3 was measured

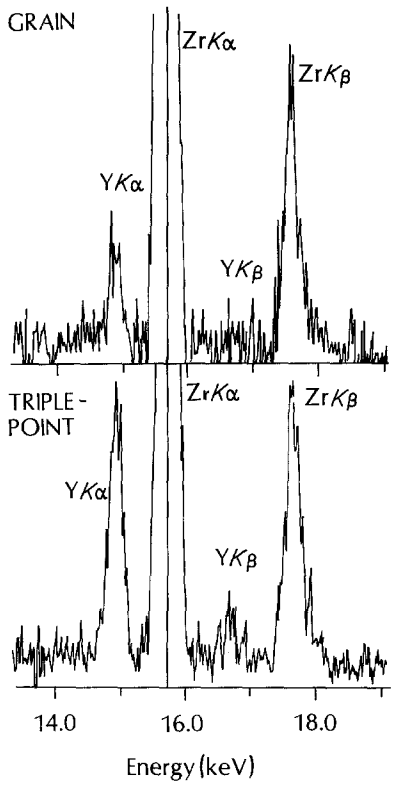

Figure 9 Part of the energy dispersive spectra showing the increase in yttrium concentration observed in the grain-boundary phase.

in this laboratory [12] and it was reported that at 400° C the observed differences, at least for these compositions, were insignificant.

In order to explain the large differences in the grain-boundary resistivity between the slowly cooled and quenched specimens one has to assume that either these, or any other chemical changes (at or near the grain boundaries) involving the grain boundary phase, occurred during cooling from the sintering temperature. A specimen cooled at the rate of TZ3Y–00A151 from the sintering temperature (1500° C) to 1300° C, held for 0.5 h to enhance chemical changes and then quenched, showed no increase in R_{gb} when compared with the TZ3Y–00A156 specimen (Fig. 4). Furthermore, rapidly cooled specimens when either (1) annealed at 900° C (11 h) or 1100° C (10 h) and then quenched (Figs 5 and 6) or (2) slowly cycled between room temperature or 350° C and a temperature ranging between 750 and 900° C showed only a small increase in the grain-boundary and volume resistivities.

Disproportionation of the TZ3Y–00A composition as a result of being in the two-phase field [7, 13], during slow cooling or annealing both within the grains and at the grain boundaries may account for small increases in the grain-boundary and volume resistivities. However, major changes in R_{gb} as a result of different cooling rates from the sintering temperature cannot be explained by the chemical processes discussed above. It appears that the grain-boundary glassy phases play a dominant role. This is further evinced by the observations of the thermal history effects on the pure Y–TZP material (PTZ3Y). The grain-boundary resistivity of this material was much lower than the Toyo Soda TZ3Y–00A154 specimen given an indentical heat treatment and was not affected by the cooling rate. Moreover, the activation energy associated with the grain-boundary resistivity is independent of the cooling rate indicating that the same mechanism is responsible for migration of oxygen ions across grain boundaries in both slowly cooled and quenched specimens. Alternative explanations, involving de-wetting of the grain boundaries, must be considered.

4.2. Relocation (or de-wetting) of grain-boundary phases

The de-wetting of grain-boundaries on cooling from the sintering temperature is not an unknown phenomenon in ceramic systems. Clarke [9, 14], in a discussion of the subject, cites as examples, the glass phase in ZnO varistors and in LiF liquid-phase sintered spinels. To explain de-wetting Clarke suggests that a variety of mechanisms are possible which may affect the balance of various forces acting at the grain-boundary interfaces giving rise to de-wetting or uniform spreading.

In our case we observe larger and more frequent glass-phase filled pockets and triple junctions in specimens which have been subjected to a quench, thus indicating preferential de-wetting of grain boundaries in these materials. The exact mechanism for de-wetting is not clear but several hypothesis can be postulated.

The microstructure of the ceramic at the sintering temperature is likely to consist of several grains of TZ3Y uniformly coated with the molten grain-boundary glassy phase. On quenching, the outer skin of the specimens will cool much more rapidly than the inner core material. Because of the tendency of the material to shrink inwards, the external surface will apply compressive forces on the core. The resulting compression may then act to drive the still mobile glassy phase in the inner region of the specimens into triple points and other low-energy sites.

If differential cooling from the interior to exterior of the sample provides the mechanism for redistribution of the grain-boundary phases, it is possible that the exterior and interior of the specimens have different grain-boundary resistivity. To examine this possibility impedance measurements were made on 0.7, 3.1 and 6.1 mm thick specimens (diameter ~ 9.6 mm), all quenched from 1500° C. Under the circumstances where the outer skin of the specimens cools much more rapidly, it would have the high-temperature microstructure frozen-in and therefore is expected to have high-grain boundary resistivity. If the thickness of the outer layer is significant, the total grain-boundary resistivity of the specimen is expected to change with increase in the volume of the material coming under compression during cooling. No significant differences in the grain-boundary resistivity data were detected between all three specimens. This null result may simply suggest that in these small grain-size materials, much thinner specimens would need to be prepared to observe any appreciable changes.

Alternatively, the possibility exists that the thermal expansion mismatch between the TZ3Y and the

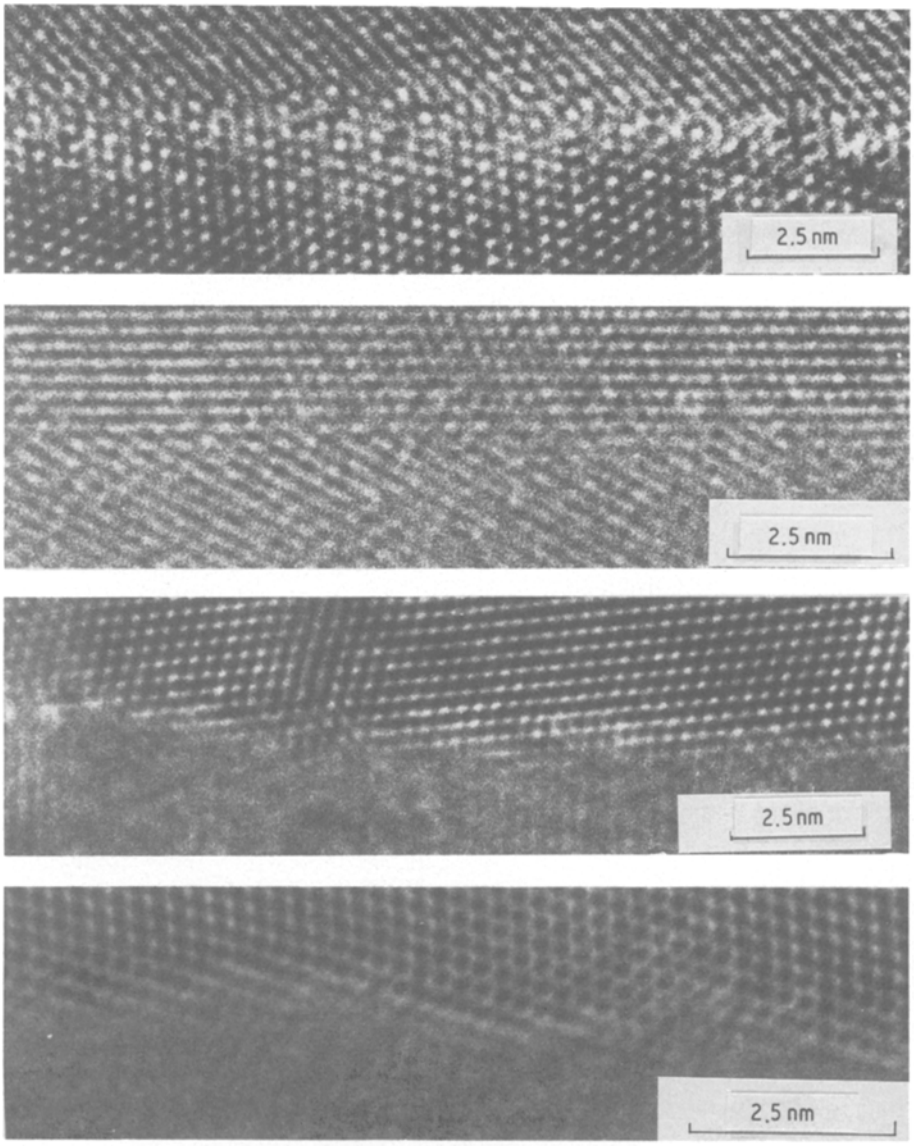

Figure 10 High-resolution electron micrographs of four different grain-boundary interfaces. Atom to atom contacts are evident in conjunction with atomic steps.

grain-boundary phase may provide the necessary driving force to redistribute more favourably the mobile grain-boundary phases. For the quenched specimens the net relative change in the thermal expansion with time is large, giving rise to high internal forces when compared with specimens subjected to slow cooling.

We believe that, due to thermal stresses, it is the relocation of the grain-boundary phase into triple points and low-energy pockets which is responsible for the observed improvements in the grain-boundary resistivity when the materials are quenched from the sintering temperature. This is further evident from the fact that (1) in TZ3Y–20A specimens where the grain-boundary phase(s) had already been removed by alumina, the change in R_{gb} as a result of different cooling rate was relatively small and (2) in low-impurity PTZ3Y specimens the cooling rate had a little effect on the grain-boundary resistivity.

Whatever the mechanism, preferential de-wetting in quenched materials relocates the glassy phase into low-energy sites resulting in less restrictive paths for the diffusing oxygen ions.

Two further reported observations require some comment: the appearance of monoclinic zirconia in the X-ray diffraction spectra of the as-fired surface of the slowly cooled material; and the increase in the Y/Zr ratio observed on the surface of the slowly cooled material measured by ESCA.

It has been reported on numerous occasions [15–17] that these materials (Y–TZP), when subjected to ageing in air at low temperatures (200 to 300° C), exhibit dramatic increases in measured monoclinic content. The variables which influence the rate of decomposition at these low temperatures are the time and temperature, the grain size and hence firing temperature, furnace atmosphere, fired density and Y_2O_3 content. We suggest that the observed higher monoclinic content in the slowly cooled materials that we observe is a result of the sample having slowly passed through the critical temperature regime at which monoclinic zirconia is known to be produced. The length of time at this temperature range is an important factor, and would explain the absence of monoclinic zirconia at the surface in the quenched materials. Further to this, the absence of monoclinic zirconia in the pure material, P–TZ3Y, and relatively low

concentration in Al_2O_3-containing specimens on slow cooling, can be explained in terms of a grain-size difference. For Toya Soda materials the presence of minor impurities, and hence a grain-boundary phase, promotes grain growth especially at the surface [10]. As a result this material will have a higher percentage of grains of a size which are more unstable with respect to the tetragonal–monoclinic phase transition.

The increased Y/Zr ratio measured on slowly cooled specimens of TZ3Y by ESCA is more puzzling. We have observed that surface chemistry of these materials is complex and have identified Y/Zr/Si/C/O/Na as the principle surface species. It is possible that the observed increase in the yttrium content at the surface of slowly cooled specimens is a consequence of the decomposition reaction which is known to occur and which was first suggested by Lange *et al.* [16]. The reaction involves the formation of α-$Y(OH)_3$ by the action of water vapour on the yttrium content of Y-TZP. This would give rise to increase in the Y/Zr ratio at the surface as detected by ESCA. We also observe an effective increase in the oxygen content at the surface along with increase in yttrium, consistent with the above hypothesis. Further work is in progress to study systematically the influence of the thermal history on the surface of these materials.

5. Conclusions

In TZ3Y materials the decrease in the grain-boundary resistivity with increased cooling rate is attributed to relocation of the grain-boundary phase rather than to chemical changes occurring at or near the grain boundaries. The relocation appears to result from thermal stresses arising either due to different thermal expansion coefficients of the grain boundary and TZ3Y phases or the skin of the specimens cooling more rapidly and applying compressive forces on the inner core material.

Acknowledgements

The authors thank F. T. Ciacchi for assistance with specimen preparation, A. Hughes for surface analysis and Dr M. V. Swain for constructive discussions.

References

1. T. K. GUPTA, F. F. LANGE and J. H. BECHTOLD, *J. Mater. Sci.* **13** (1978) 1464.
2. S. P. S. BADWAL and M. V. SWAIN, *J. Mater. Sci. Lett.* **4** (1985) 487.
3. J. DRENNAN and S. P. S. BADWAL, Proceedings of the 3rd International Conference on the Science and Technology of Zirconia (1986). Advances in Ceramics, Vol. 24, Science and Technology of Zirconia III (The American Ceramic Society, Westerville, Ohio) in press.
4. S. RAJENDRAN, J. DRENNAN and S. P. S. BADWAL, *J. Mater. Sci. Lett.* **6** (1987) 1431.
5. S. P. S. BADWAL, *J. Electroanal. Chem.* **202** (1986) 93.
6. C. A. LEACH and P. TANEV and B. C. H. STEELE, *J. Mater. Sci. Lett.* **5** (1986) 893.
7. M. RÜHLE, N. CLAUSSEN and A. H. HEUER, "Advances in Ceramics", Vol. 12, edited by N. Claussen, M. Rühle and A. H. Heuer (The American Ceramic Society, Columbus, Ohio, 1984) p. 352.
8. A. H. HEUER, *J. Amer. Ceram. Soc.* **70** (1987) 689.
9. D. R. CLARKE, *J. de Physique* **46** (1985) C4-51.
10. R. CHAIM, D. G. BRANDON and A. H. HEUER, *Acta Metall.* **34** (1986) 1933.
11. R. CHAIM, A. H. HEUER and D. G. BRANDON, *J. Amer. Ceram. Soc.* **69** (1986) 243.
12. S. P. S. BADWAL, *J. Mater. Sci. Lett.* **6** (1987) 1419.
13. H. G. SCOTT, *J. Mater. Sci.* **10** (1975) 1527.
14. D. R. CLARKE, *Ann. Rev. Mater. Sci.* **17** (1987) 57.
15. T. SATO, S. OHTAKI and M. SHIMADA, *J. Mater. Sci.* **20** (1985) 1466.
16. F. F. LANGE, G. L. DUNLOP and B. I. DAVIS, *J. Amer. Ceram. Soc.* **69** (1986) 237.
17. S. ITO and M. WATANABE, Proceedings of Zirconia '86, Tokyo, Japan (1986). Advances in Ceramics, Vol. 24, Science and Technology of Zirconia III (The American Ceramic Society, Columbus, Ohio) in press.

Received 28 December 1987
and accepted 4 May 1988